

NUMERICAL BASIS OF CAD-EMBEDDED CFD

Dr. A. Sobachkin, Dr. G. Dumnov, (Mentor Graphics Corporation, Mechanical Analysis Division, Russia)

Dr. A. Sobachkin, Engineering Manager

THEME

CAD CAE Integration: Meshing & Integration of Analysis into the Design Process

SUMMARY

FloEFD is a new class of CFD (Computational Fluid Dynamics) analysis software (called Concurrent CFD) that is fully embedded in the mechanical design environment, for all general engineering applications. FloEFD was developed by Mentor Graphics' Mechanical Analysis Division, which is one of the top three CFD vendors in the world today and the leader in multiCAD-embedded CFD.

All CFD software includes a representation of the Navier-Stokes equations, turbulence models and models for physical phenomena. Since the early 1980s CFD codes have grown in complexity, particularly in physical modelling, but with less emphasis on dealing with geometric complexity. In parallel, mechanical CAD systems have become the backbone of the product creation process in almost all industry sectors, allowing very complex geometries to be constructed with relative ease. In 1999, SolidWorks introduced the first version of FloWorks, providing for the first time a CFD simulation capability inside a MCAD system, directly using native CAD geometry without modification as the starting point for the CFD process. Since then a number of CAD-embedded and CAD-associated tools have appeared. These tools use different numerical technologies to traditional CFD ranging from mesh generation to differencing schemes and wall treatment, yet not much has been published about their inner workings. This paper takes an in-depth look under the hood at the numerical basis for one such tool – FloEFD.

The idea is underpinned by the choice of meshing technology in FloEFD and the impact that choosing a Cartesian-based mesh has on the way the geometry is handled, in particular solid-fluid and solid-solid interfaces, the wall treatment used to capture boundary layer evolution, and calculation of skin friction and heat fluxes. A specific challenge is the treatment of thin walls and multilayer shells.

NUMERICAL BASIS OF CAD-EMBEDDED CFD

Finally, we show how the rectilinear mesh and boundary layer models have been extended by a set of physical models covering: real gases; supersonic and hypersonic flows; gas/gas premixed and non-premixed combustion; boiling; cavitation and condensation processes. Radiation models that account for spectral characteristics will also be briefly presented.

KEYWORDS

CAE, CFD, EFD, FloEFD, CAD-embedded, mesh, meshing technology, numerical schemes, solver technology, engineering analysis, engineering fluid dynamics, multiphysics.

1: INTRODUCTION

In modern design practice, product lifecycle management concepts (PLM) are widely deployed by engineers in many industries as the means by which 3D manufactured product data are used and maintained consistently during an entire product's lifecycle and across all its design changes. The basis of a PLM concept is the availability of high-quality, complete, detailed, and accurate 3D product model data within a mechanical CAD system as the central element. 3D product model data are therefore both the foundation and starting point for all virtual prototyping and physical simulations today. The use of fluid flow simulations using Computational Fluid Dynamics (CFD) in such a CAD-embedded context is obviously very attractive, as it can not only accelerate the design process, but make these processes more predictable and reliable, against a background of increasing design complexity and dependence on external development partners. It is essential to note that all major CAD systems were created some time ago and were optimized as a design tools. Only later was the necessity of embedded CAE (and in particular CFD) recognized. Moreover, CAE and CFD tools already have a long history during which they have been optimized for their respective tasks. Therefore it was logical that for some period CFD continued as an independent development, and interaction with CAD was limited by simple data exchange. Nevertheless from the standpoint of using CFD during design, and as a requirement of all PLM roadmaps the need to fully embed CFD within CAD becomes more and more pressing. At the end of the 1990s the first fully-embedded CFD product, FloWorks, was developed as an add-in for SolidWorks. Later this product became the starting point for the Mentor Graphics' FloEFD suite of products for different CAD systems based on an Engineering Fluid Dynamics (EFD) approach. The solver and mesher is used not only for FloEFD, but has been re-packaged as an enabling technology for a new stand-alone product, FloTHERM XT, dedicated to electronics cooling applications.

The EFD approach is based on 2 main principles:

- Direct use of native CAD as the source of geometry information;
- Combination of full 3D CFD modelling with simpler engineering methods in the cases where the mesh resolution is insufficient for full 3D simulation.

Since the EFD technology has to operate within different CAD systems it was developed as a universal CAD/CFD platform that incorporates a number of technologies:

- CAD data management;
- Mesh generation;
- Several CFD solvers;
- Engineering Modelling Technologies; and
- Results processing

NUMERICAL BASIS OF CAD-EMBEDDED CFD

The CAD/CFD platform forms the bridge between CAD system and CAD-embedded CFD products, like FloEFD, or alternatively provides an API for vertically-specialized CFD products like FloTHERM XT to make use of all the relevant functions of a solid modelling engine (see Fig. 1):

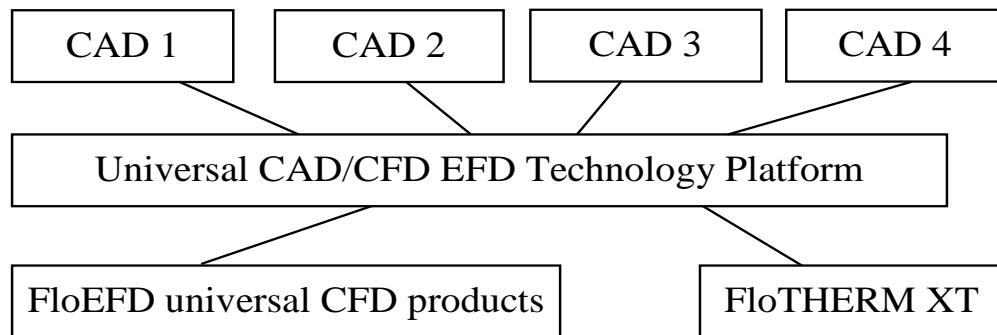


Figure 1: Universal EFD Platform Technology as a bridge between CAD and CFD.

2: EFD BOUNDARY TREATMENT

CAD describes the solid model, whereas CFD is primarily concerned with the flow space (the solution domain minus the solid model). Historically, for traditional CFD codes, the fluid space is created by Boolean subtraction of the solid model within the CAD system, and this inverse solid passed to the CFD tool for meshing. Mesh generators in traditional CFD are usually based on body-fitted algorithms. The detailed reviews of basic types of mesh geometries are presented in several publications (e.g. Weatherill & Hassan, 1994, Filipiak, 1996 and Parry & Tatchell, 2008). In these works it is shown that body-fitted meshes have been widely used for solving industrial problems. As a rule, for complicated geometries unstructured meshes are used, formed by constructing irregularly distributed nodes (see Fig. 2a). Where the geometries being meshed are less complex it is often possible to use structured meshes (see Fig. 2b), and these two meshing strategies can be combined, with structured meshes in some sub-regions, e.g. close to walls, and unstructured meshes everywhere else (see Fig. 2c). Such meshes may be called partially structured or partially unstructured.

CAD systems were originally developed solely with design in mind, and not numerical simulation. A characteristic of body-fitted meshes is that they are highly sensitivity to the quality (for simulation purposes, not necessarily for design) of the CAD geometry. Usually such meshes are generated beginning from nodes generation at solid surface. Then the surface is meshed by means of Delaunay triangulation. After that, based on the surface triangulation, the space mesh is generated. Often it is a mesh with tetrahedral elements that meet

Delaunay criterion (e.g. Delaunay, 1934, Lawson, 1977, Watson 1981, Baker, 1989 and Weatherill & Hassan, 1994). In many cases, defects in the surface representation require user intervention to resolve the ambiguities to heal the defects in the CAD geometry. In addition, in some situations over-refinement of the surface can result in an excessive number of small triangles. This can happen in areas that are not significant in terms of flow simulation as the meshing algorithm responds to geometry features (small radii, small spikes, material joints etc.) requiring the user to take remedial action.

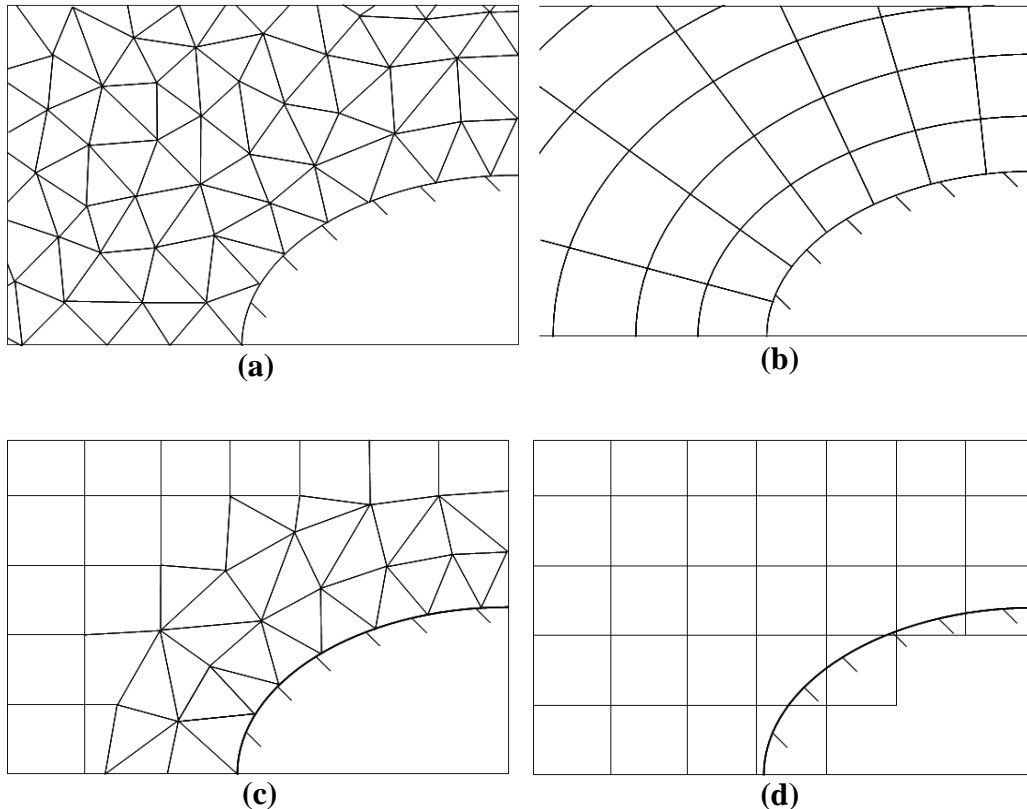


Figure 2: Unstructured body fitted mesh (a), structured body-fitted mesh (b), combination of structured Cartesian mesh and non-structured body-fitted mesh near the wall (c) and structured Cartesian immersed-body mesh (d)

The alternative approach is to use an immersed-body mesh as it shown in Fig. 2d. In this approach the creation of the mesh starts independently from geometry itself and the cells can arbitrarily intersect the boundary between solid and fluid. This makes it possible to use a Cartesian-based mesh, which in the general case cannot be body-fitted. Such a mesh can be defined as a set of cuboids (rectangular cells), which are adjacent to each other and to the external boundary of the computational domain, orientated along the Cartesian coordinates. Cuboids intersected by the surface (“cut-cells”) are treated in a special way, described later, according to the boundary conditions defined on the surface. It is necessary to point out that the immersed body mesh approach

NUMERICAL BASIS OF CAD-EMBEDDED CFD

can be implemented for tetrahedral and other types of the elements (see Löhner et al., 2004), but in terms of approximation accuracy and ease of implementation, Cartesian meshes are strongly preferred.

Advantages of Cartesian meshes can be summarized as follows:

- Simplicity, speed and robustness of the mesh generation algorithm especially when dealing with native CAD data;
- Minimization of Local Truncation Errors (Mentor Graphics, 2011a); and
- Robustness of the differential scheme.

The EFD technology is based upon the use of Cartesian-based meshes and Meshing Technology is one of the key elements of the CAD/CFD bridge for CAD-embedded CFD.

As a result of using Cartesian-based meshes we have cells which are located fully in solid bodies (solid cells), in the fluid (fluid cells) and cells intersected the immersed boundary (which we term 'partial cells'). In the simplest case the partial cell consists from 2 control volumes (CV): a fluid CV and a solid CV (see Fig 3).

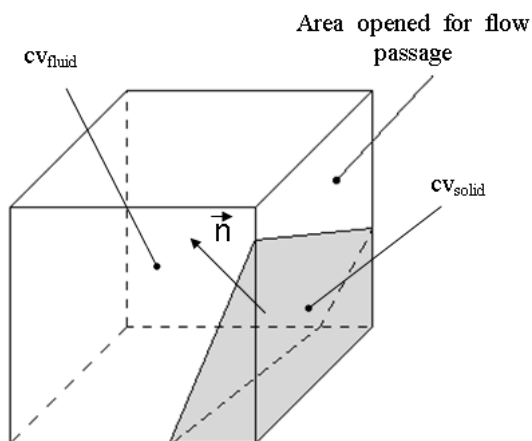


Figure 3: Partial cell in the simplest case and with 2 control volumes (CV) inside.

Each CV is then fully solid or fully fluid. For each CV all necessary geometrical parameters such as volume and the coordinates of cell centre are calculated. The areas and normal vector direction are calculated for the faces that bounds the CV. All these data are taken directly from the native CAD model. Moreover, the direct use of the native CAD model allows all aspects of the geometry within the partial cell to be specified (e.g. solid edges) – see Fig. 4. Here the CAD/CFD bridge technology takes into account the points C_1 C_2 on the solid edge in order to describe in mesh representation the 2 facets: $A_1-C_1-C_2-A_2$ and $B_1.C_1-C_2-B_2$ which correspond exactly to the 2 facets in the CAD model.

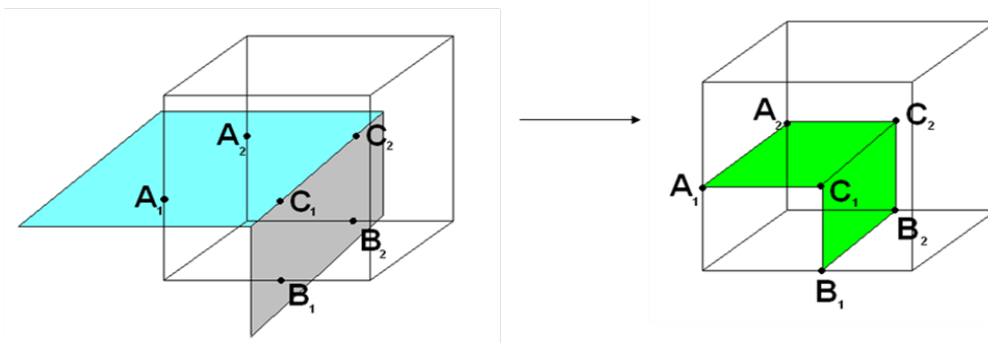


Figure 4: Representation of CAD geometry (left) in the partial cell (right) in case of 2 facets and solid edge inside one cell.

Such technology allows good resolution of geometry features even in case of relatively coarse meshes (see Fig. 5).

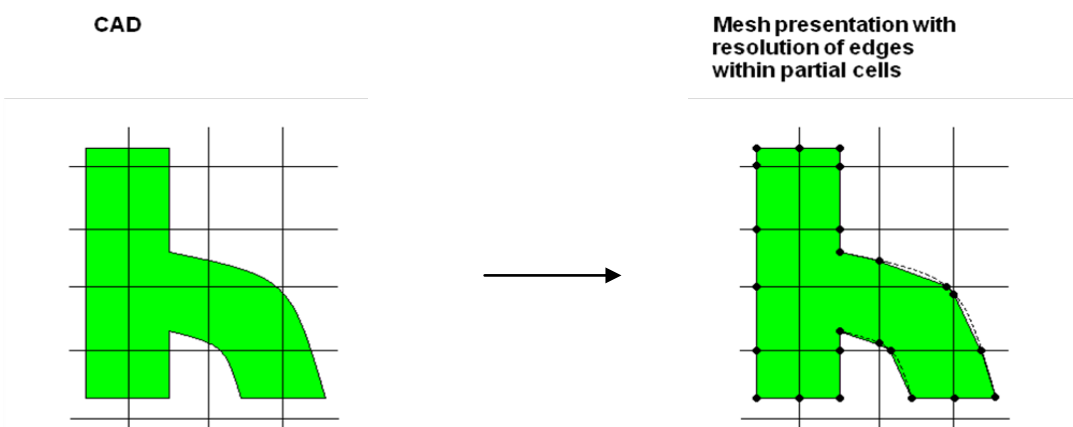


Figure 5: Mesh representation of CAD geometry with resolution of solid edges within partial cells.

Within one single cell it is possible to have an arbitrary number of CVs: 3 in case of one thin wall or more, as shown in Fig. 6.

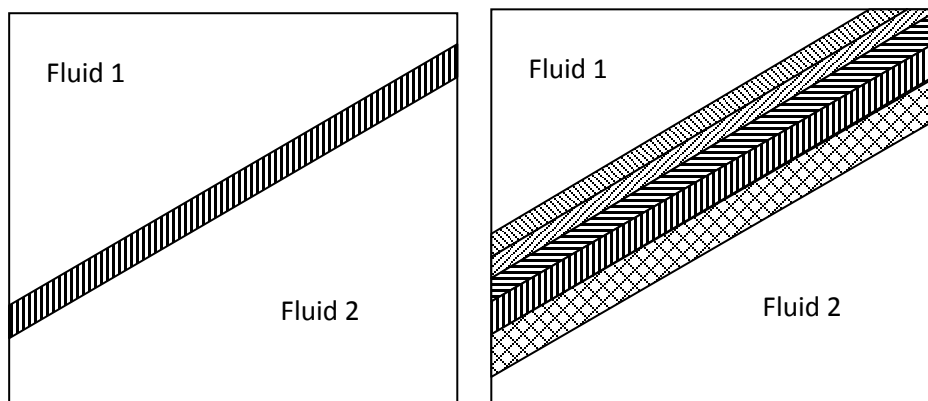


Figure 6: Partial cell with 3 control volumes (fluid-solid-fluid) in case of thin solid wall and partial cell with 7 control volumes in case of thin solid wall having inside 5 layers with different material properties.

NUMERICAL BASIS OF CAD-EMBEDDED CFD

Multiple layers of CVs are essential not only for fluid flow modelling but for heat transfer phenomena, including the contact resistances and Joule heating calculations within a solid body (a fully-coupled multiphysics application). The solid and fluid CVs can be alternated many times within each cell as presented in Fig. 7.

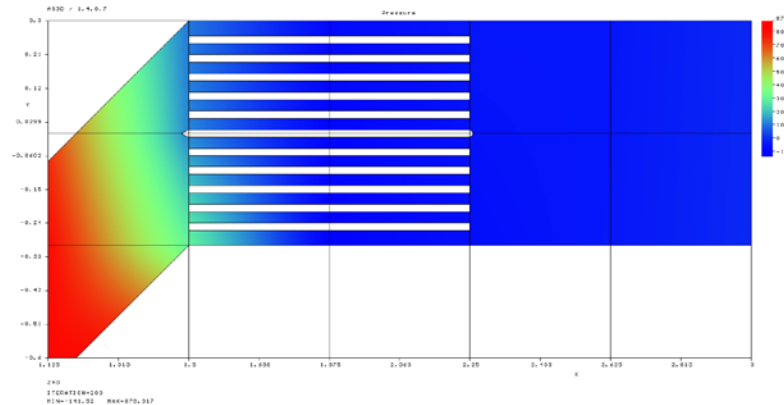


Figure 7: Multiple control volumes (solid-fluid-solid-fluid-.. etc.) for partial cells.

Mesh generation is started by dividing the rectangular computational domain into a set of rectangular cells (cuboids) formed by intersection of planes parallel to the axes of coordinate system. The mesh can be refined (by splitting each cuboid into 8 geometrically-similar cuboids) using various adaptation criteria that can be defined for each solid body (curvature, narrow channels, small features, etc.) and automatically according to gradients in the solution.

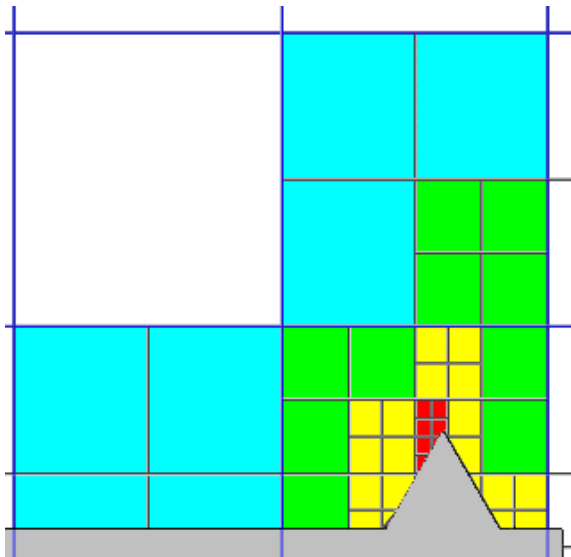


Figure 8: EFD mesh after refinement.

Due to refinement, cells having different refinement level are formed, it is essential to note that the difference in refinement level for neighbouring cells in the EFD technology is not more than 1, as shown in Fig. 8.

These refinement procedures are essential to resolve features of the CAD geometry like surfaces with small curvature, small features, narrow channels, etc. Moreover, the use of such mesh generation technology allows the implementation of efficient and robust automatic tools for meshing. The input data required can be only the size of the geometric object (which can be taken from CAD automatically), the size of the smallest feature to be resolved and some general information about the task (internal or external flow, choice of physical models to be used, etc.). It is also possible to activate additional refinement of the mesh during the calculation, with the goal of better adaptation of the mesh to singularities in the solution like shock waves.

3: PHYSICAL MODELS

In general the Cartesian mesh approach used in FloEFD allows to be performed conjugate multiphysics calculations, using one computation mesh having fluid cells, solid cells and (multi-CV) partial cells:

- Fluid flow analysis for fluid regions;
- Heat transfer and direct electrical current calculation in solid regions.

Fluid flow analysis and thermal conduction can also be treated separately. In addition, all these calculations can be coupled with different radiation models. For all these physical phenomena the native CAD geometry remains the source of initial geometric information.

1. Fluid regions

In fluid regions FloEFD solves the Navier-Stokes equations, which are formulations of mass, momentum and energy conservation laws:

$$\frac{\partial \rho}{\partial t} + \frac{\partial(\rho u_i)}{\partial x_i} = 0 \quad (1)$$

$$\frac{\partial(\rho u_i)}{\partial t} + \frac{\partial}{\partial x_j}(\rho u_i u_j) + \frac{\partial P}{\partial x_i} = \frac{\partial}{\partial x_j}(\tau_{ij} + \tau_{ij}^R) + S_i \quad (2)$$

$$\frac{\partial \rho H}{\partial t} + \frac{\partial \rho u_i H}{\partial x_i} = \frac{\partial}{\partial x_i} \left(u_j (\tau_{ij} + \tau_{ij}^R) + q_i \right) + \frac{\partial p}{\partial t} - \tau_{ij}^R \frac{\partial u_i}{\partial x_j} + \rho \varepsilon + S_i u_i + Q_H \quad (3)$$

$$H = h + \frac{u^2}{2}$$

NUMERICAL BASIS OF CAD-EMBEDDED CFD

For calculation of high speed compressible flows and flows with shock waves the following energy equation is used:

$$\frac{\partial \rho E}{\partial t} + \frac{\partial \rho u_i \left(E + \frac{P}{\rho} \right)}{\partial x_i} = \frac{\partial}{\partial x_i} \left(u_j (\tau_{ij} + \tau_{ij}^R) + q_i \right) - \tau_{ij}^R \frac{\partial u_i}{\partial x_j} + \rho \varepsilon + S_i u_i + Q_H \quad (4)$$

$$E = e + \frac{u^2}{2}$$

These equations are supplemented by fluid state equations defining the nature of the fluid, and by empirical dependencies of fluid density, viscosity and thermal conductivity on temperature. Inelastic non-Newtonian fluids are considered by introducing a dependency whereby their dynamic viscosity is dependent on flow shear rate and temperature.

Special models are used for the description of real gases, volume condensation and vaporization, cavitation, combustion as well as for porous media.

FloEFD is able to consider both laminar and turbulent flows. Laminar flows occur at low values of the Reynolds number, which is defined as the product of representative scales of velocity and length divided by the kinematic viscosity. When the Reynolds number exceeds a certain critical value the flow transitions smoothly to turbulent. To predict turbulent flows, the Favre-averaged Navier-Stokes equations are used, where time-averaged effects of the flow turbulence on the flow parameters are considered, whereas the large-scale, time-dependent phenomena are taken into account directly. Through this procedure, extra terms known as the Reynolds stresses appear in the equations for which additional information must be provided. To close this system of equations, FloEFD employs transport equations for the turbulent kinetic energy and its dissipation rate, using the k - ε model.

The modified k - ε turbulence model with damping functions proposed by Lam and Bremhorst (1981) describes laminar, turbulent, and transitional flows of homogeneous fluids consisting of the following turbulence conservation laws:

$$\frac{\partial \rho k}{\partial t} + \frac{\partial \rho k u_i}{\partial x_i} = \frac{\partial}{\partial x_i} \left(\left(\mu + \frac{\mu_t}{\sigma_k} \right) \frac{\partial k}{\partial x_i} \right) + \tau_{ij}^R \frac{\partial u_i}{\partial x_j} - \rho \varepsilon + \mu_t P_B, \quad (5)$$

$$\frac{\partial \rho \varepsilon}{\partial t} + \frac{\partial \rho \varepsilon u_i}{\partial x_i} = \frac{\partial}{\partial x_i} \left(\left(\mu + \frac{\mu_t}{\sigma_\varepsilon} \right) \frac{\partial \varepsilon}{\partial x_i} \right) + C_{\varepsilon 1} \frac{\varepsilon}{k} \left(f_1 \tau_{ij}^R \frac{\partial u_i}{\partial x_j} + C_B \mu_t P_B \right) - f_2 C_{\varepsilon 2} \frac{\rho \varepsilon^2}{k} \quad (6)$$

$$\tau_{ij} = \mu s_{ij}, \quad \tau_{ij}^R = \mu_t s_{ij} - \frac{2}{3} \rho k \delta_{ij}, \quad s_{ij} = \frac{\partial u_i}{\partial x_j} + \frac{\partial u_j}{\partial x_i} - \frac{2}{3} \delta_{ij} \frac{\partial u_k}{\partial x_k}, \quad (7)$$

$$P_B = -\frac{g_i}{\sigma_B} \frac{1}{\rho} \frac{\partial \rho}{\partial x_i}, \quad (8)$$

where $C_\mu = 0.09$, $C_{\varepsilon 1} = 1.44$, $C_{\varepsilon 2} = 1.92$, $\sigma_k = 1$, $\sigma_\varepsilon = 1.3$, $\sigma_B = 0.9$, $C_B = 1$ if $P_B > 0$, $C_B = 0$ if $P_B < 0$, the turbulent viscosity is determined from:

$$\mu_t = f_\mu \cdot \frac{C_\mu \rho k^2}{\varepsilon}, \quad (9)$$

Lam and Bremhorst's damping function f_μ is determined from:

$$f_\mu = \left(1 - e^{-0.025 R_y}\right)^2 \cdot \left(1 + \frac{20.5}{R_t}\right), \quad (10)$$

Where:

$$R_y = \frac{\rho \sqrt{k} y}{\mu}, \quad (11)$$

$$R_t = \frac{\rho k^2}{\mu \varepsilon}, \quad (12)$$

y is the distance from point to the wall and Lam and Bremhorst's damping functions f_1 and f_2 are determined from:

$$f_1 = 1 + \left(\frac{0.05}{f_\mu}\right)^3, \quad f_2 = 1 - e^{-R_t^2}. \quad (13)$$

Lam and Bremhorst's damping functions f_μ , f_1 , f_2 decrease turbulent viscosity and turbulence energy and increase the turbulence dissipation rate when the Reynolds number R_y based on the average velocity of fluctuations and distance from the wall becomes too small. When $f_\mu = 1$, $f_1 = 1$, $f_2 = 1$ the approach reverts back to the original k - ε model.

The heat flux is defined by:

$$q_i = \left(\frac{\mu}{\text{Pr}} + \frac{\mu_t}{\sigma_c}\right) \frac{\partial h}{\partial x_i}, \quad i = 1, 2, 3 \quad (14)$$

Here the constant $\sigma_c = 0.9$, Pr the Prandtl Number, and h is the thermal enthalpy.

A particular computational task is finally specified by the definition of its geometry, boundary and initial conditions. All data for such conditions are defined directly on the native CAD model.

NUMERICAL BASIS OF CAD-EMBEDDED CFD

2. Solid regions

FloEFD calculates two kinds of physical phenomena within solid regions: heat conduction and direct electrical current, with the resulting Joule heating being a source of heat in the energy equation.

Heat transfer in solids and fluids with energy exchange between them (conjugate heat transfer) is an essential and implicit element of CAD-embedded CFD software. Heat transfer in fluids is described by the energy equation (3-4) where the heat flux is defined by (14). The phenomenon of heat conduction in solid media is described by the following equation:

$$\frac{\partial \rho e}{\partial t} = \frac{\partial}{\partial x_i} \left(\lambda_i \frac{\partial T}{\partial x_i} \right) + Q_H \quad (15)$$

where e is the specific internal energy, $e = c \cdot T$, c is specific heat, Q_H is specific heat release (or absorption) rate per unit volume, and λ_i are the eigenvalues of the thermal conductivity tensor. It is supposed that the heat conductivity tensor is diagonal in the considered coordinate system. For an isotropic medium $\lambda_1 = \lambda_2 = \lambda_3 = \lambda$. In presence of electric current, Q_H may include the specific Joule heat release Q_J . It is defined as $Q_J = r \cdot j^2$, where r is the electrical resistivity and j is the electric current density. The electric current density vector:

$$\mathbf{i} = - \left(\frac{1}{r_{11}} \frac{\partial \phi}{\partial x_1}, \frac{1}{r_{22}} \frac{\partial \phi}{\partial x_2}, \frac{1}{r_{33}} \frac{\partial \phi}{\partial x_3} \right) \quad (16)$$

is determined via the electric potential $\phi[V]$ from the steady-state Laplace equation:

$$\frac{\partial}{\partial x_i} \left(\frac{1}{r_{ii}} \frac{\partial \phi}{\partial x_i} \right) = 0 \quad (17)$$

Here r_{ii} is the temperature-dependent electrical resistivity in the i -th coordinate direction.

The Laplace equation is solved numerically in sub-domains that contain electrically conductive materials. Dielectric solids and fluid areas inside such sub-domains are automatically excluded. The total electric current over a surface $I[A]$ or electric potential $\phi[V]$ may be specified by the user as a boundary condition for the problem.

A surface between two electrically-conductive solids in the sub-domain is either considered zero-resistance (the default) or the user can specify an electrical contact resistance on it. The resistance value is either given explicitly or calculated directly from the given material and its thickness. A contact resistance specified on a surface implies that the current passing through it produces the corresponding Joule heating, which gives rise to a surface heat source, as follows.

If a solid consists of several solid materials attached to each other, then the thermal contact resistances between them are taken into account when calculating the heat conduction. As a result, a solid temperature step appears on the contact surfaces. A very thin layer of another material between solids or on a solid in contact with fluid can be taken into account when calculating the heat conduction in solids in the same manner (i.e. as a thermal contact resistance), but is specified via the material's thermal conductivity and the layer thickness.

The energy exchange between the fluid and solid media is calculated via the heat flux in the direction normal to the solid/fluid interface taking into account the solid surface temperature and the fluid boundary layer characteristics, and radiation heat exchange if necessary.

3. Radiation between solid surfaces and in transparent solids

Radiation is a complex phenomena and therefore there are a lot of simplified models of radiation. All of them have advantages, disadvantages and limitations. FloEFD includes 2 models:

- 1) Ray Tracing, also known as DTRM (Discrete Transfer Radiation Model).
- 2) Discrete Ordinates (or DO).

For the Ray Tracing model the heat radiation from solid surfaces, both the emitted and reflected, is assumed diffuse (except for symmetry and mirror radiative surface types), i.e. they obey Lambert's law, according to which the radiation intensity per unit area and per unit solid angle is the same in all directions. Solar radiation is absorbed and reflected by surfaces independently from thermal radiation. Thermal radiation passes through a solid specified as radiation transparent without any absorption. A solid can be specified as transparent to the solar radiation only, or transparent to the thermal radiation from all sources except the solar radiation, or transparent to both types of radiation: thermal and solar. Refraction can also be taken into account for this option. Fluids neither emit nor absorb thermal radiation (i.e. they are transparent to the thermal radiation), so the thermal radiation affects solid surfaces only. Radiative solid surfaces not specified as a blackbody or white body are assumed to be an ideal gray body, i.e. having a continuous emissive power spectrum similar to that of a blackbody, so their monochromatic

NUMERICAL BASIS OF CAD-EMBEDDED CFD

emissivity is independent of the emission wavelength. For certain materials with certain surface conditions, the gray body emissivity can depend on the surface temperature. Spectrum dependency isn't taken into account in the Ray Tracing model.

The Discrete Ordinates model is more complicated. Here the whole 4π directional domain at any location within the computational domain is discretized into the specified number of equal solid angles. Radiation governing equation can be written as follows:

$$\frac{dI(\vec{s}, \vec{r})}{ds} = -(\kappa + \sigma_s) \cdot I(\vec{s}, \vec{r}) + \kappa \cdot n^2 \cdot I_b(\vec{r}) + \frac{\sigma_s}{4\pi} \int_{\Omega'=4\pi} \Phi(\vec{s}', \vec{s}) \cdot I(\vec{s}', \vec{r}) \cdot d\Omega' \quad (18)$$

Radiation absorptive (semi-transparent) solids absorb and emit thermal radiation in accordance with the specified solid material's absorption coefficient. Scattering is not considered. Surfaces of opaque solids absorb the incident thermal radiation in accordance with their specified emissivity coefficients, the rest of the incident radiation is reflected specularly or diffusively, or both specularly and diffusively, in accordance with the specified specularity coefficient. Radiation is refracted in accordance with the specified refraction indices of the solid and adjacent medium (another radiation absorptive solid, or a transparent solid or fluid, the refraction index of which is always considered as equal to 1). The radiation spectrum is considered as consisting of several bands, the edges of which are specified by the user. Properties of radiation sources, surfaces and materials are considered constant within each band.

As the result of radiation calculations the appropriate heat fluxes are taking into account in partial cells for immersed fluid-solid boundaries or in solid cells inside the semi-transparent solid bodies.

4: BOUNDARY LAYER TREATMENT

Non body-fitted Cartesian meshes appear optimal for managing the native CAD data, and so form the basis for the CAD/CFD bridge. The main issue for Cartesian immersed-body meshes is the resolution of boundary layers on coarse meshes. For this the EFD technology incorporates an original approach described below, and the combination of this approach with the EFD Cartesian mesh technology forms a major part of EFD CAD/CFD bridge.

Consideration of the near-wall cells shows that for arbitrary native CAD geometry the mesh between the solid/fluid boundary can be too coarse for the accurate solution of Navier-Stokes equations within the high-gradient

boundary layer. Therefore, in order to calculate skin friction and heat flux at the wall, the Prandtl approach for boundary layers is used. The key idea of this approach has some similarity with the wall function approach traditionally used in CFD. The wall treatment that forms part of the EFD platform technology uses a novel and original Two-Scale Wall Function (2SWF) approach (Mentor Graphics, 2011b) that consists of two methods for coupling the boundary layer calculation with the solution of the bulk flow:

- 1) A “thin” boundary layer treatment that is used when the number of cells across the boundary layer is not enough for direct, or even simplified, determination of the flow and thermal profiles; and
- 2) A “thick” boundary layer approach when the number of cells across the boundary layer exceeds that required to accurately resolve the boundary layer.
- 3) In intermediate cases, a compilation of the two above approaches is used, ensuring a smooth transition between the two models as the mesh is refined, or as the boundary layer thickens along a surface.

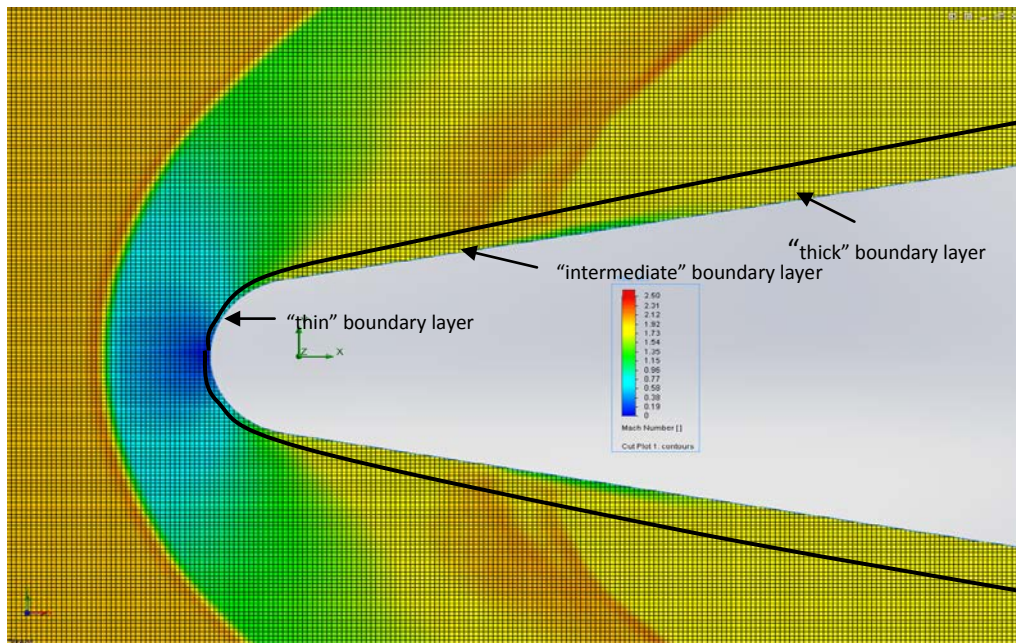


Figure 9: Mach Number flow field with “thin”, “intermediate” and “thick” viscous boundary layer.

Verifications of the EFD technology boundary layer treatment were done by Balakine et al. (2004). These treatments are discussed below.

1. The Thin-Boundary-Layer approach

In the thin-boundary-layer approach the Prandtl boundary layer equations already integrated along the normal to the wall (i.e. along the normal to body surface ordinate) from 0 (at the wall) to the boundary layer thickness δ are solved along fluid streamlines covering the walls. If the boundary layer is

NUMERICAL BASIS OF CAD-EMBEDDED CFD

laminar, these equations are solved with a method of successive approximations based on the Shvets trial functions technology (Ginzburg, 1970). If the boundary layer is turbulent or transitional, a generalization of this method employing the Van Driest hypothesis about the mixing length in turbulent boundary layers is used (Van Driest, 1956).

The influence of roughness, considered as the equivalent sand grain roughness, and the external flow's turbulence on the boundary layer are modeled through semi-empirical coefficients correcting the wall shear stress and the heat flux from the fluid to the wall. Fluid compressibility, turbulence kinetic energy dissipation, and various body forces are also taken into account through corresponding empirical and semi-empirical models.

From the boundary layer calculation FloEFD obtains the boundary layer thickness δ , the wall shear stress τ_w^e , and the heat flux from the fluid to the wall q_w^e , which are used as boundary conditions for the Navier-Stokes equations:

$$\tau_w = \tau_w^e, \quad q_w = q_w^e, \quad (19)$$

Boundary conditions for k and ε are determined from the condition of turbulence equilibrium in the near-wall computational mesh cell:

$$\frac{\partial k}{\partial y} = 0, \quad \varepsilon = \frac{C_\mu^{0.75} k^{1.5}}{\kappa y}. \quad (20)$$

2. The Thick-Boundary-Layer approach

When the number of cells across the boundary layer is sufficient (more than ~ 10) the simulation of laminar boundary layers is done via Navier-Stokes equations as part of the core flow calculation. For turbulent boundary layers a modification of the well-known wall function approach is used. However, instead of the classical approach where the logarithmic velocity profile is used, the EFD technology uses the full profile proposed by Van Driest (1956):

$$u^+ = \int_0^{y^+} \frac{2 \cdot d\eta}{1 + \sqrt{1 + 4 \cdot \kappa^2 \cdot \eta^2 \cdot \left[1 - \exp\left(-\frac{\eta}{A_v}\right) \right]^2}} \quad (21)$$

where $\kappa = 0.4054$ is the Karman constant, $A_v = 26$ is the Van Driest coefficient.

All other assumptions are similar ones to the classical wall function approach.

5: NUMERICAL METHODS AND COMPUTATIONAL EXAMPLES

The fluid region represents the main computational challenge from the point of view of algorithmic complexity and of calculation overhead. Using arbitrary CAD as a source of geometric information, it is essential to pay specific attention to the robustness and efficiency of the numerical methods used.

FloEFD uses 3 different types of solver and related numerical algorithms for modeling fluid flows. The first solver is optimal for incompressible flows and flows with Mach Numbers less than 3.0. Time-implicit approximations of the continuity and convection/diffusion equations (for momentum, temperature, etc.) are used together with an operator-splitting technique (see Glowinski and Tallec, 1989, Marchuk, 1982, Samarskii, 1989, Patankar, 1980). This technique is used to efficiently resolve the problem of pressure-velocity decoupling. Following a SIMPLE-like approach (Patankar, 1980), an elliptic type discrete pressure equation is derived by algebraic transformations of the originally-derived discrete equations for mass and momentum, taking into account the boundary conditions for velocity.

To solve the asymmetric systems of linear equations that arise from approximations of momentum, temperature and species equations, a preconditioned generalized conjugate gradient method from Saad (1996) is used. Incomplete LU factorization is used for preconditioning.

To solve the symmetric algebraic problem for pressure-correction, an original double-preconditioned iterative procedure is used. It is based on a specially-developed multigrid method from Hackbusch (1985).

The example below is based on the use of this first type of solver. This is an external flow around a F-16 fighter (Mach Number equals 0.6 and 0.85). The geometry is a native CAD model of the airplane with external tanks and armaments. Flow into the intake and exhaust from the engine's nozzle are both taking into account.

Calculations were performed with approximately 200,000 cells, showing the efficiency of EFD technology. Calculation results are compared with the test data from Nguyen, Luat T. et al. (1979).

NUMERICAL BASIS OF CAD-EMBEDDED CFD

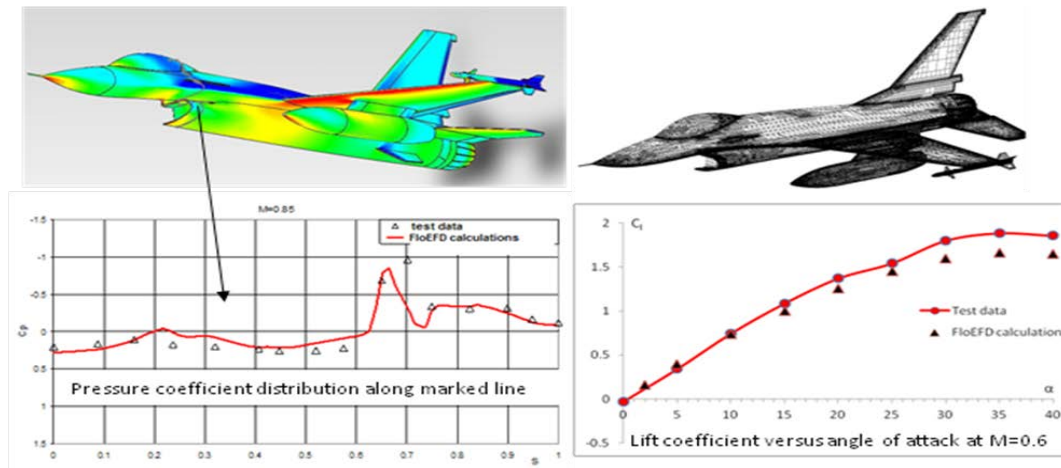


Figure 10: Fighter Airplane F-16 calculation.

This solver is extended by the broad set of physical models available for FloEFD like gravitation, radiation, real properties of various fluid media, combustion, phase transfer, etc. Presented below are some examples that illustrate some of these capabilities. The first example shows the modeling of the combustion processes in vortex combustor shown in Fig 11.

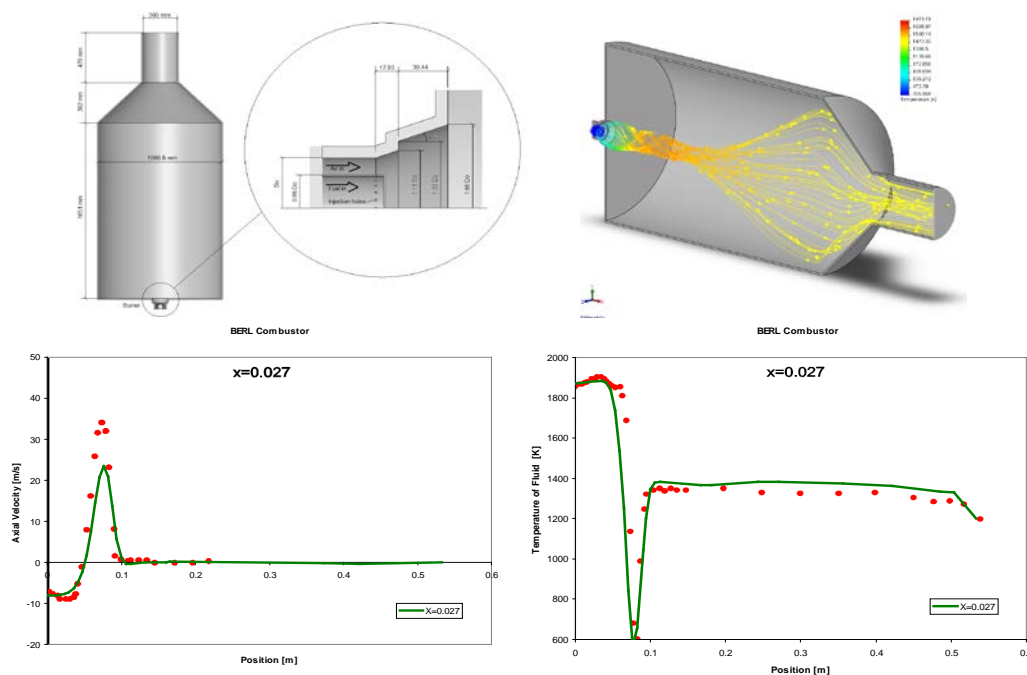


Fig. 11: Vortex combustor (natural gas/air).

Here calculation examples are compared with experimental data from Sayre et al. (1994). This example also shows the efficiency of the technology for cases having geometry with differing characteristic dimensions.

Use of the EFD technology platform as a CAD/CFD bridge brings additional benefits for the resolution of specific flows in dedicated elements of complex models where the number of cells is not enough for full 3D modeling. Having direct access to the native CAD data, the EFD technology platform can recognize that some geometry can form flow passages akin to pipes or thin channels, because this information exists in the CAD system. In such cases, analytical or empirical data is used to replace the 3D Navier Stokes equation modeling within such flow passages. In Fig. 12 such an approach is presented for the flow within a pin fin heatsink.

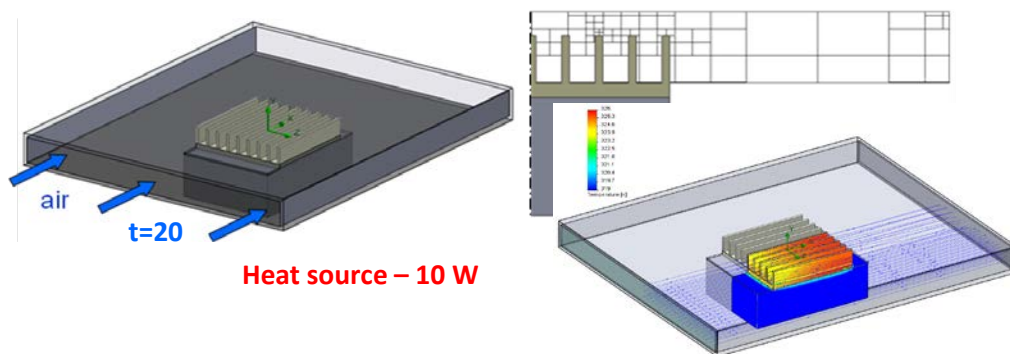


Figure 12: FloEFD calculation using “Thin channel” technology.

Here the abovementioned thin channel technology is used, where the number of cells across the channel was 1-2. FloEFD calculation results for a very coarse mesh (3,900 cells in a total) and a relatively fine mesh (180,000 cells in a total) with comparison against experimental data from Jonsson and Palm, (1998) are presented in Table 1.

Flow velocity	0.9 m/s		1.3 m/s		1.6 m/s		1.9 m/s	
$R_{t,exp}$ K/W	3.72		3.20		2.91		2.69	
Cells number	3,900	180,000	3,900	180,000	3,900	180,000	3,900	180,000
$R_{t,calc}$ K/W	3.714	3.77	3.213	3.22	2.969	2.93	2.78	2.70
δ , %	0.2	1.3	0.4	0.6	2	0.7	3.3	0.3

Table 1. FloEFD calculation results using “Thin channel” approach (3,900 cells), full 3D approach (180,00) cells and its difference with experiment.

Calculation of an air conditioning device containing Freon R22 as the working fluid shows the benefits of the same approach for a far more complicated model (see Fig 13).

NUMERICAL BASIS OF CAD-EMBEDDED CFD

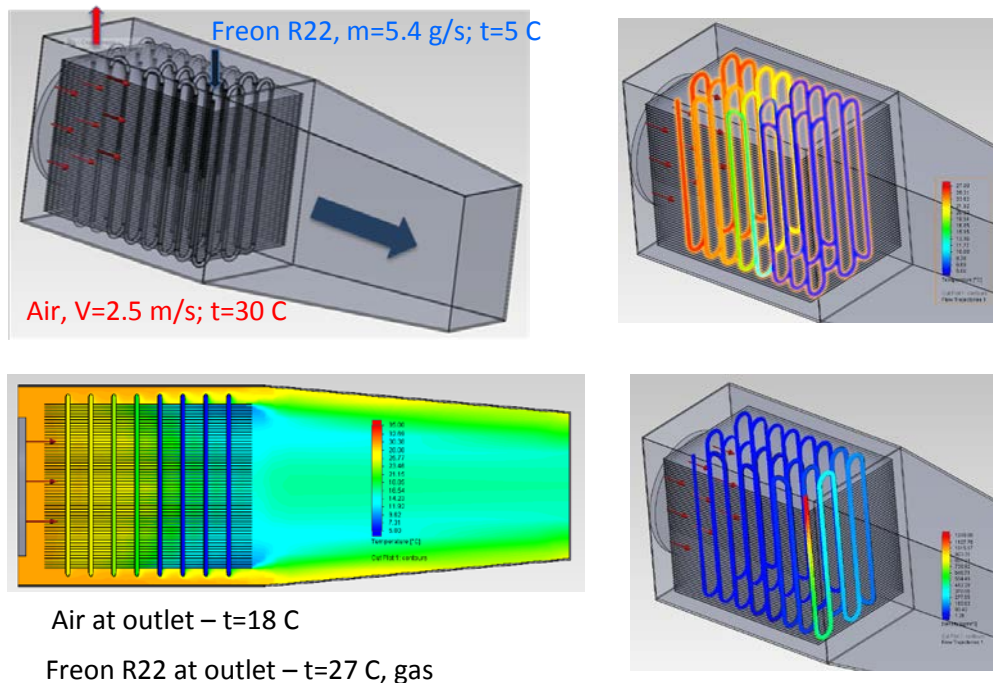


Figure 13: Air condition operation simulation

In this case, heat exchange in the solid and phase exchange processes in the Freon are both taken into account.

The second solver is optimal for High Mach number tasks with shock waves and other related phenomena. This explicit numerical solver (see Gavrilouk et al., 1993) is based on modification of Godunov method (see Samarscii, 1989). This solver is also used in FloEFD for modeling of hypersonic flows of air with Mach Number up to 30, by taking into account the phenomena of air ionization and dissociation. In Fig. 14, the calculation example presented shows the flow around a blunt-nosed cylinder and comparison of calculation results with the experimental data of Gaitonde and Shang, 1993.

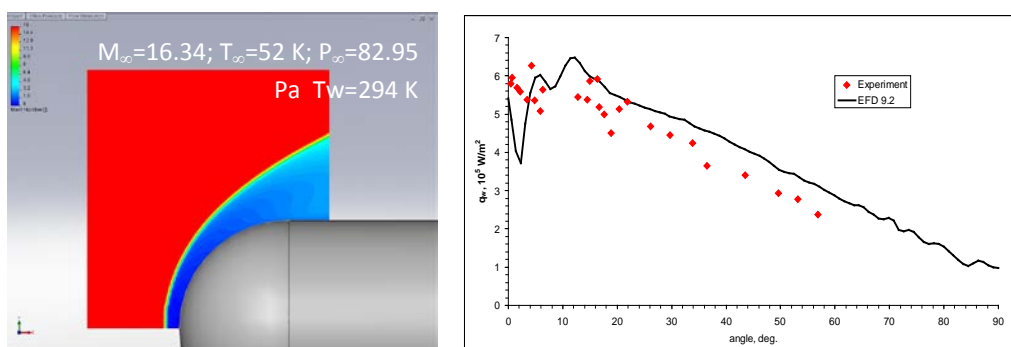


Figure 14: Hypersonic flow around blunt - nose cylinder.

The third recently-proposed solver in FloEFD is used for the calculation of flows in liquids with cavitation, using a numerical approach that is essentially

new for CFD (see Alexandikova et al., 2011). The phenomena of cavitation presents a lot of numerical difficulties concerned with variations of density, speed of sound and time scale. The speed of sound may drop from thousands of meters per second in liquid flow to order ten or less in vaporized flow. This can lead to supersonic flows with high Mach numbers, sometimes with shocks. Cavitation problems are thereby characterized by wide range of Mach number from near zero to several tens within a single calculation domain. Therefore, when constructing a numerical method to simulate cavitating flows, it is important to take into account the fact that regions of incompressible flow and highly compressible flow coexist in the calculation domain.

To date there are two main approaches to calculating such all-speed compressible flows. The first one employs the “density-based” methods originally developed to simulate speed compressible flows. These methods are adapted for low Mach number cases by introducing artificial compressibility or using some preconditioning techniques (Kunz et al., 2000, Lee et al., 2006, 2007).

The second approach utilizes the “pressure-based” methods originally developed for incompressible flows. Usually these are the SIMPLE-family of differencing schemes (or “pressure-correction” methods) and adapted for the cases involving compressible flows at high speed (van der Heul et al., 2000).

FloEFD’s approach differs from both of the above. At first glance the idea to apply the “pressure-based” in regions of incompressible flow and the “density-based” approach in regions of supersonic compressible flow looks quite natural. But it is not obvious how to couple these approaches. We propose a way of combining the approaches that is based on the following simple key idea. Employing the finite-volume method, we suggest mixing the fluxes and pressure approximations that correspond to “pressure-based” and “density-based” approaches on the faces of control volumes. After that, these mixed approximations are substituted in a SIMPLE-type differencing scheme. Managing the mixing weight between the fluxes and pressure approximation, we can obtain either the original SIMPLE-type semi-implicit splitting scheme or the explicit “density-based” scheme or a mixture of these approaches.

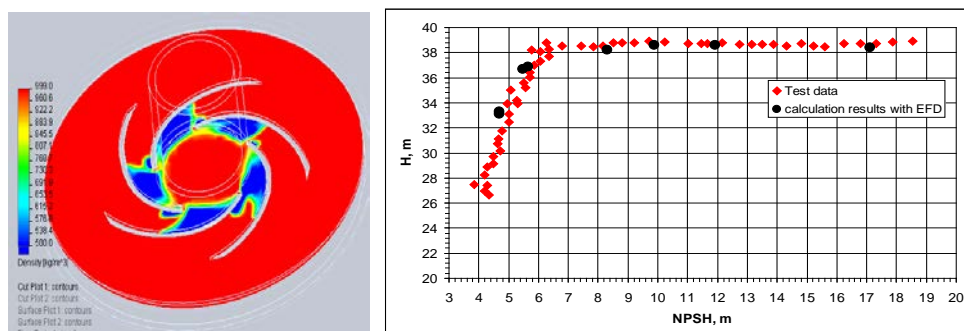


Figure 15. Calculation of cavitation in centrifugal pump.

NUMERICAL BASIS OF CAD-EMBEDDED CFD

Figure 15 shows an example of flow in a centrifugal pump, with cavitation captured using this hybrid solver. The FloEFD calculation results are compared with experimental data by Hofman et al. (2001).

6: CONCLUSIONS

Trends in the worldwide CAE market clearly shows steady growth in the market share of CFD calculations in the solution of up-to-date design problems. Within this market, FloEFD is an innovative example of the adaptation of up-to-date CAE technology (namely fluid dynamics and heat transfer) for the everyday needs of design engineers.

EFD (Engineering Fluid Dynamics) Technology has been developed as a universal CAD/CFD platform, which consists the following technologies: managing with CAD data, Cartesian-based mesh generator, a set of CFD solvers, Engineering Modelling Technologies, and result processing. Such platform becomes a complete bridge between CAD and CFD.

EFD Technology is based on the following key principles:

- Cartesian-based meshing technology, directly dealing with arbitrary complex native CAD geometry;
- Boundary Layer treatment technology that allows fluid flow calculations to be performed on relatively coarse Cartesian-based meshes. This technology is based on a fully scalable wall function approach to define skin friction and heat flows at solid walls; and
- Engineering Models, employed when the computational mesh is not fine enough for full 3D modelling.

The paper presents calculation examples using all 3 types of CFD solvers used in FloEFD: an implicit solver for incompressible and low compressible flows; an explicit solver for high Mach Number and hypersonic flows; and hybrid solver for liquid flows with cavitation, thus demonstrating both the high simulation efficiency and the high accuracy of the EFD technology. This combination of good performance for relatively coarse meshes, CAD-embedded capability, and a high level of automation and usability regarding the model set up, meshing and solution make FloEFD an effective CFD tool for analysis in support of engineering design.

REFERENCES

- Alexandrikova T., Pavlov A., Streltsov V. (2011) Hybrid density- and pressure-based splitting scheme for cavitating flows simulation, *Computational Methods in Multiphase Flow VI*, Editors: A.A. Mammoli, C.A. Brebbia, WIT Transactions on Engineering Sciences, Vol. 70, pp 41-56, WIT Press, 2011, ISBN: 978-1-84564-518-2.
- Baker, T.J. (1989) Automatic Mesh Generation for Complex Three-Dimensional Regions Using a Constrained Delaunay Triangulation, *Engineering with Computers*, Vol. 5, pp.161-175.
- Balakin, V., Churbanov, A., Gavrioliouk, V., Makarov, M. and Pavlov A. (2004) Verification and Validation of EFD.Lab Code for Predicting Heat and Fluid Flow, *Proceedings of ICHMT International Symposium on Advances in Computational Heat Transfer*, Norway, April 19-24, 2004.
- Delaunay, B.N. (1934) Sur la Sphere Vide. *Izvestia Akademia Nauk SSSR, VII Seria, Otdelenie Matematicheskii I Estestvennyka Nauk*, Vol. 7 pp.793-800.
- Filipiak, M. (1996) *Mesh Generation*, Edinburgh Parallel Computing Centre, The University of Edinburgh, Version 1.0, November 1996.
- Ginzburg, I.P. (1970) *Theory of Drag and Heat Transfer*. Leningrad, LGU (in Russian).
- Gaitonde D., Shang J.S. (1993) Accuracy of flux – split algorithms in high – speed viscous flows, *AIAA Journal*, Vol.31 No. 7 pp. 1215-1221.
- Gavriliouk, V.N. Denisov, O.P. Nakonechny, V.P. Odintsov, E.V. Sergienko, A.A. Sobachkin, A.A. (1993) Numerical Simulation of Working Processes in Rocket Engine Combustion Chamber, *44th Congress of the international Astronautical Federation*, IAFF-93-S.2.463, October 16-22, Graz, Austria.
- Glowinski, R. and P. Le Tallec (1989) *Augmented Lagrangian Methods and Operator-Splitting Methods in Nonlinear Mechanics*. SIAM, Philadelphia.
- Hackbusch, W. (1985) *Multi-grid Methods and Applications*, Springer-Verlag, NY, USA.
- Hofman M., Stoffel D., Coutier-Delgosha O., Fortes-Platella R., Reboud JI. (2001) *Experimental and numerical studies on a centrifugal pump with 2D-curved blades in cavitation condition*, CAV2001:session B7.005.
- Jonsson, H. and B. Palm, (1998) Thermal and Hydraulic Behavior of Plate Fin and Strip Fin Heat Sinks under Varying Bypass Conditions, *Proc. 1998*

NUMERICAL BASIS OF CAD-EMBEDDED CFD

InterSociety Conf. on Thermal and Thermomechanical Phenomena in Electronic Systems (ITHERM '98), IEEE, pp. 96-103, ISBN 0.7803-4475-8.

Kunz R., Boger D., Stinebring D., Thomas S. Chyczewski, Lindau J., Gibeling H., Venkateswaran S., Govindan T. (2000) A preconditioned Navier-Stokes method for two-phase flows with application to cavitation prediction, *Computers & Fluids*, Volume 29, Issue 8, 31 August 2000, Pages 849-875.

Lam, C.K.G. and Bremhorst, K.A. (1981) Modified Form of Model for Predicting Wall Turbulence, *ASME Journal of Fluids Engineering*, Vol.103, pp. 456-460.

Lawson, C.L. (1977) Software for C1 Surface Interpolation, *Mathematical Software III*, pp.161-194.

Li Ding, Charles L. Merkle (2006) A unified framework for incompressible and compressible fluid flows, *Journal of Hydrodynamics*, Ser. B, Volume 18, Issue 3, Supplement 1, Proceedings of the Conference of Global Chinese Scholars on Hydrodynamics, July 2006, Pages 113-119

Li Ding, Xia Guoping, Merkle Charles L. (2007) Consistent properties reconstruction on adaptive Cartesian meshes for complex fluids computations, *Journal of Computational Physics*, Volume 225, Issue 1, 1 July 2007, Pages 1175-1197

Lohner, R. Cebral, J. Castro, M. Baum, J.D. Luo, H. Mestreau, E. and Soto, O. (2004) Adaptive Embedded Unstructured Grid Methods, *Mecanica Computacional*, Vol. XXIII, pp. 29-42, G.Buscaglia, E.Dari, O.Zamonsky (Eds.), Bariloche, Argentina, November.

Marchuk, G.I. (1982) *Methods of Numerical Mathematics*, Springer-Verlag, Berlin.

Mentor Graphics (2011a) Advanced Immersed Boundary Cartesian Meshing Technology in FloEFD™, MGC 02-11, TECH9690-w, Mentor Graphics Corporation, 2011.

Mentor Graphics (2011b) Enhanced Turbulence Modeling in FloEFD™, MGC 02-11, TECH9670-w, Mentor Graphics Corporation, 2011.

Nguyen, Luat T. et al. (1979) Simulator Study of Stall/Post – Stall Characteristics of a Fighter Airplane with Relaxed Longitudinal State Stability, *NASA Technical Paper 1538*, Dec. 1979.

Parry, J. and Tatchell, D. (2008) Flomerics' EFD Meshing Technology: A White Paper, Flomerics Ltd.

Patankar, S.V. (1980) *Numerical Heat Transfer and Fluid Flow*, Hemisphere, Washington, D.C.

Saad, Y. (1996) *Iterative methods for sparse linear systems*, PWS Publishing Company, Boston.

Samarskii, A.A. (1989) *Theory of Difference Schemes*, Nauka, Moscow (in Russian).

Sayre A,N. Lallemand, J. Dugue, R. Weber (1994) Scaling Characteristics of Aerodynamics and Low-NOx Properties of Industrial Natural Gas Burners, *The SCALING 400 Study, Part IV: The 300 kW BERL Test Results*, IFRF Doc No F40/y/11, International Flame Research Foundation, The Netherlands.

Watson, D.F. (1981) Computing the Delaunay Tesselation with Application to Voronoi Polytopes. *The Computer Journal*, Vol. 24(2) pp. 167-172.

Van der Heul D.R., Vuik C., Wesseling P. (2002) A conservative pressure-correction method for flow at all speeds. J.M. Burgers Center, Department of Applied Mathematical Analysis, Faculty of Information Technology and System, Delft University of Technology, Mekelweg 4, 2628 CD Delft, The Netherlands, 2002.

Van der Heul Duncan R., Vuik C. and Wesseling P. (2000), Efficient computation of flow with cavitation by compressible pressure, European Congress on Computational Methods in Applied Sciences and Engineering, ECCOMAS 2000.

Van Driest, E.R. (1956) On Turbulent Flow Near a Wall, *Journal of the Aeronautical Science*, Vol. 23, No. 10, pp. 1007.

Weatherill N.P. and Hassan O. (1994) Efficient Three-dimensional Delaunay Triangulation with Automatic Point, *International Journal for Numerical Methods in Engineering*, Volume 37, Issue 12, pp 2005–2039, 30 June 1994